Alexandria Journal of Science and Technology

Article

Synthesis and AC Electrical Characterization of Isobutylene Isoprene Rubber Loaded with Carbon Black Fillers

Khaled Alfaramawi*, Sayed Abboudy, Laila Abulnasr, Omar Salah

Department of Physics, Faculty of Science, Alexandria University, Alexandria 21511, Egypt.

* *Correspondence Address:*

Khaled Alfaramawi: Department of Physics, Faculty of Science, Alexandria University, Alexandria 21511, Egypt. Email address: kalfaramawi@alexu.edu.eg.

KEYWORDS: IIR rubber, HAF, GPF, Composites, carbon black, Aggregates.

Received:
May 02, 2025
Accepted:
June 03, 2025
Published:
July 04, 2025

ABSTRACT: Isobutylene isoprene rubber (IIR) filled with High Abrasion Furnace (HAF) and General-Purpose Furnace (GPF) carbon black nano fillers was synthesized and characterized. The fillers were embedded in the rubber matrix with various concentrations (40, 60, 70, 80 and 100 phr), The thermal stability of the synthesized composites was examined by thermogravimetric analysis (TGA). The surface morphology of the samples was analyzed using scanning electron microscopy (SEM). It was observed that the carbon black particles were assembled in aggregates which are randomly distributed among the rubber matrix. The size of the aggregates was greatly influenced by the amount of filler content. The AC electrical conductivity of the composites was investigated as a function of frequency at different temperatures. The frequency-dependent conductivity followed Jonscher's power law and hence, the frequency exponent was estimated for all samples. Moreover, the correlated barrier hopping model was used to calculate the maximum barrier height. In addition, the frequency- dependent dielectric constant of the rubber/carbon black composites was studied.

1. INTRODCTION

Polymers have been recognized as insulators primarily due to the inherent characteristics of covalent bonds, which form the majority of the bonding within polymers. Butyl rubber is a copolymer which is normally synthesized from approximately 98% of isobutylene and 2% of isoprene. Hence, it is denoted as IIR [1]. Polymers lack the ability to supply free electrons for electrical conduction and are unable to function as a path for electrical charges movement. Hence, they are considered to be electrically insulating and have been utilized accordingly in various applications. However, with the advent of technological advancements, the demand for electrically conductive polymers has become increasingly significant due to their diverse range of uses [2]. These include materials for electromagnetic interference shielding, dissipation of static electric charges, spark-proof rubber contact switches, pressure-sensitive sensors, and semiconducting materials in high voltage cables and ultra sonic transducers [3, 4]. As a result, the preparation of conducting polymers and the enhancement of their electrical properties have gained considerable importance over the time.

The addition of metallic powders, flakes, whiskers, and other conducting fillers like carbon black (CB), as an amorphous carbon allotrope, and graphite (carbon crystalline allotrope) into an insulating rubber matrix is a highly effective technique for creating an interconnected carrier path [5-7]. A particularly innovative method in the field of polymer science and engineering involves incorporating carbon black CB into the polymer matrix to produce conducting polymeric materials [8, 9]. The conductive path is established by the charge carriers within the insulating matrix, leading to the formation of a conductive path. The characteristics are strongly influenced by the structure and type of both the polymer and carbon black components [10-13]. The interaction between CB fillers themselves within the composite plays a crucial role in creating three-dimensional aggregation structures within the rubber matrix. This allows carriers to move between aggregates.

Many studies on rubber/carbon black composites reached a conclusion that a substantial proportion of high aspect ratio of carbon black filler results in the creation of a network structure within the composite material [14-20]. Others have examined the processes of dielectric response in polymeric systems, and the electrical relaxation [21].

In the present study, Isobutylene isoprene rubber (IIR) filled with High Abrasion Furnace (HAF) and General Purpose

Alexandria Journal of Science and Technology, 2025, **3**(1), 99–108
Online ISSN: 2974-3273

DOI: 10.21608/AJST.2025.352064.1061

Furnace (GPF) carbon black nano fillers was synthesized and characterized. The structure was studied by scanning electronic microscope (SEM) and thermal gravimetric analysis (TGA) measurements. Moreover, the AC electrical properties of such samples were investigated. The electrical characterization includes the dependence of the electrical conductivity and dielectric response on both frequency and temperature.

2. Experimental Method

In this study, the primary matrix employed was IIR rubber. As a filler, HAF and GPF carbon blacks were incorporated into the rubber at various weight ratios, specifically 40, 60, 70, 80, and 100 phr (parts per hundred parts of rubber) by weight. Stearic acid with 2 phr is used as a lubricant. Zinc oxide (ZnO) is added with 5 phr to the rubber to activate sulfur vulcanization and thereby reduce the vulcanization time. As a processing aid, Paraffinic oil with 60 phr is used. A 3 phr of $\overline{\boldsymbol{Z}}\boldsymbol{K}^{\boldsymbol{B}}$ (Dispergum zinc soaps which is a special combination of zinc and potassium soaps) is used as an effective additive for compounds with light fillers and also to improve filler dispersion and reduce reagglomeration. IPPD4020 (N-isopropyl N'-cyclohexyl paraphenylene diamine) with 1 phr is used as antioxidant/Antiozonant. Sulphur (S) with 3 phr is used as a vulcanizing agent. The samples coding and carbon black concentrations are listed in Table 1.

The mixing process followed the Compounds and Preparing Standard Vulcanized Sheets (ASTM D 3182). To achieve homogeneity, the contents were combined using two roll mills of 150 mm in diameter and 300 mm length at a speed of 18 rpm with a gear ratio of 1.4. After being left for 24 hours, the vulcanization process took place using an electrically heated platen hydraulic press at a temperature of 150 ± 2 ℃ and pressure of 15 MPa for a duration of 15 minutes.

To investigate the morphology of the ready samples, rubber sheet is made. It is square shaped, 1cm side length and 1 mm thickness.

Thermogravimetric analysis (TGA) measurements were performed for all samples using an SDT-Q600 Simultaneous (TGA / DSC) within differential temperature readings from ambient to 200 °C at a heating rate of 5 °C/min. Scanning Electron Microscopy (SEM) [type: JSM-IT200 SEM microscope] was used to study the surface morphology of the samples. Prior to SEM examination, the samples were coated with silver using an ion sputter coater (model: JFC-1100E ion sputter).

Table 1: Sample coding and the carbon black filler contents in units of phr.

Sample code	HAF40	GPF40	HAF60	GPF60	HAF70	GPF70	HAF80	GPF80	HAF100	GPF100
HAF CB	40	-	60	-	70	-	80	-	100	-
GPF CB	-	40	-	60	-	70	-	80	-	100

AC electrical measurements of the samples were performed in the temperatures from 25 up to 120 °C ± 1 °C and frequencies from ~ 10^2 to 10^5 Hz using AC Keithley 3321 LCZ Meter Bridge. All electrical measurements were taken using disc-shaped samples. Newley fresh samples were used for electrical measurements. The surfaces of the samples were painted with conductive carbon paste. A non-inductive electric oven was employed to monitor the temperature.

3. Results and Discussion

The stability of the prepared rubber/carbon black composite samples was studied by thermogravimetric analysis. The TGA thermographs for both HAF and GPF series of samples were demonstrated in **Figures 1&2** respectively. The TGA figures show slightly mass loss by increasing of the temperature from room temperature (25 °C) up to almost 200°C.

The loss in mass in this range of temperature (~ 1.2 %) is probably attributed to evaporation of volatile constituents and/or the residual washing liquids used before the thermal measurements. It is easily noticed that IIR/CB composites are highly stable, in the investigated range of temperature. This is probably due to the fact that the vulcanizing agents would not be affected by elevation of temperature range below 200 ºC.

The morphology of the prepared samples was investigated by SEM which is frequently used to examine the distribution of the fillers in rubber matrix. SEM data of IIR/HAF CB and IIR/GPF CB samples are shown in **Figures 3&4** respectively, with resolution of 6000X. **Figures 3&4** revealed that both HAF and GPF carbon black particles are imbedded in the rubber matrix in the form of aggregates. On the other hand, the carbon black aggregates are dispersed randomly among the rubber matrix. The aggregates may tend to make agglomerates to be physically held together to establish carbon black chains inside rubber.

AC electrical measurements were carried out as a function of frequency at different temperatures. **Figures 5&6** demonstrate the relationship between the AC electrical conductivity and frequency of IIR/HAF and IIR/GPF composite samples respectively at some selected temperatures.

Figures 5&6 show, obviously, that the AC conductivity (σ_{ac}) tends to a finite value at low frequencies (DC limit) while it grows up as the frequency is increased. As a normal practice, the general behavior of the AC conductivity with the angular frequency (ω) is described by the well-known power law of Jonscher as;

$$\sigma_{ac}(\omega) = A\,\omega^{S} \qquad (1)$$

where A is a temperature dependent constant and S is the frequency exponent that was found by many researchers in similar systems to be within the range of $0.0 < S \leq 1$ [22]. The exponent S for the present samples was obtained from the data of **Figures 5&6** by plotting ln σ_{ac} versus ln ω. **Figure 7** displays explicit relationships between (ln σ_{ac}) against (ln ω) for samples HAF 40, HAF 70, GPF 60 and GPF 100 at some selected temperatures while the temperature dependance of the exponent S is shown explicitly in **Figure 8**.

The behavior of σ_{ac} with the frequency is due to charge carriers' jump across the polymer chain by hopping via the defect sites. A variety of theoretical frameworks, include classical hopping and quantum mechanical tunneling of charge carriers, have been proposed to elucidate the ac conduction behavior in rubber/filler systems [22]. In the electron tunneling model the parameter S is independent of T, while in the case of tiny polaron tunneling,

S grows up as *T* increases.

The trend of *S* with *T* for the present systems is displayed in **Figure 8**. It was noticed that *S* decreases with increasing of the temperature for all the samples. The low values of exponent $S < 0.8$ suggest that the simple pair approximation (SPA) model [23] is incapable of explaining the observed data. The SPA model is originally based on the assumption that the distance to a third site for hopping is much greater than the distance inside the pair of sites.

The Correlated Barrier Hopping (CBH) model has been employed to clarify the observed decrease in Pike [23] initially conceptualized this phenomenon for the case of single-electron hopping, subsequently refined by Elliott [24] for the scenario involving simultaneous two-electron hopping. According to the CBH model, carrier mobility is attributed to the process of hopping over the Coulomb barrier that divides two defect centers [23]. The frequency exponent *S* for this model is given by;

$$s = 1 - \frac{6k_BT}{[W_m + k_BT\, ln(\omega\tau_0)\,]} \quad (2)$$

where τ_0 is the effective relaxation time, T is the absolute temperature, k_B is Boltzmann constant and W_m is the maximum barrier height at infinite interstatic separation. In the audio frequency range, ignoring the term $[k_BT\, ln(\omega\tau_0)]$, we can get a simpler form as

$$1 - s = \frac{6k_BT}{W_m} \quad (3)$$

Figure 9 shows the relation between (1-*S*) and temperature. It is clear that there is almost linear increase in (1-*S*) by increasing temperature. Taking linear fit, W_m was calculated and listed in Table 2. It has to be mentioned that such behavior was already observed in spinel magnetic ferrites [25], and even in typical semiconductors [26-29].

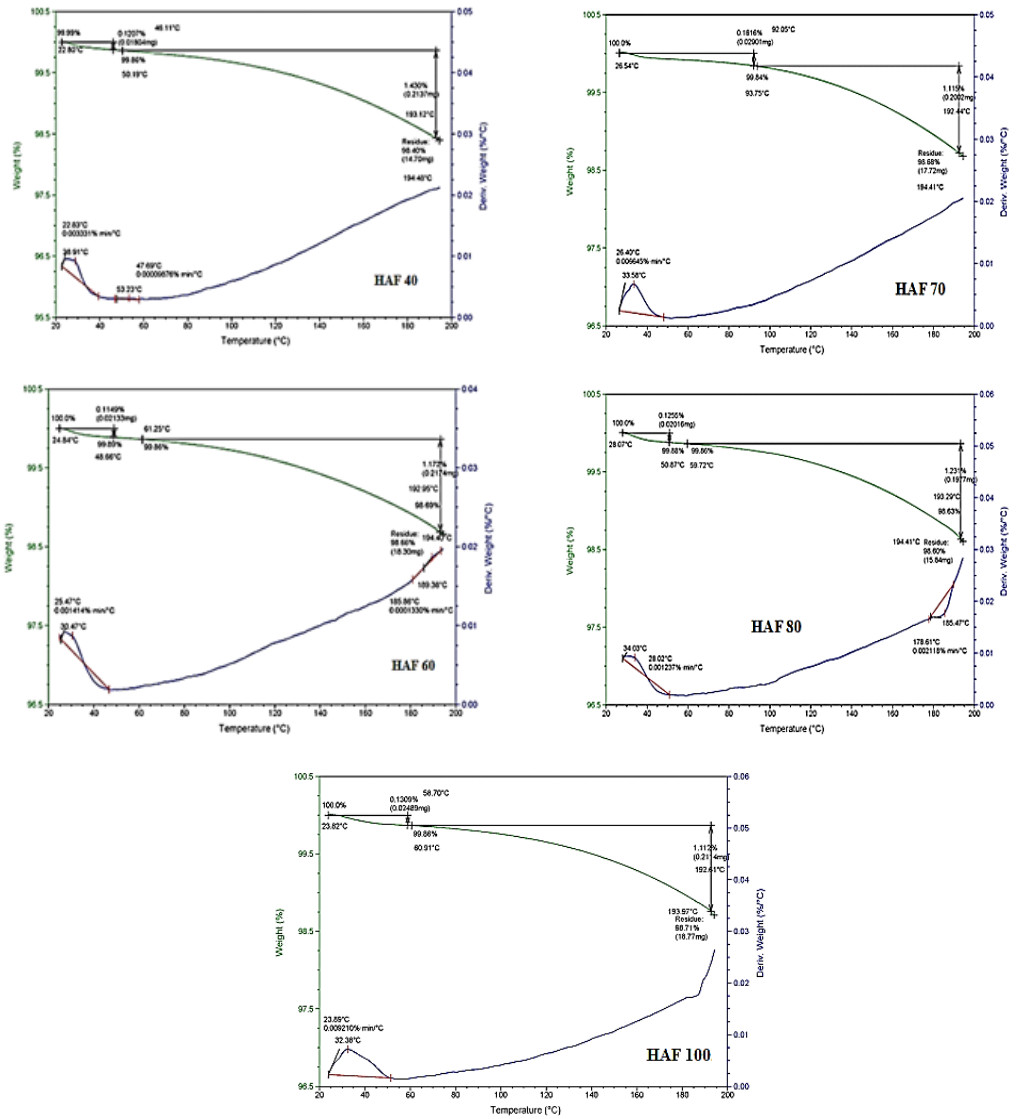

Figure 1. TGA thermographs for IIR/ HAF CB composite samples.

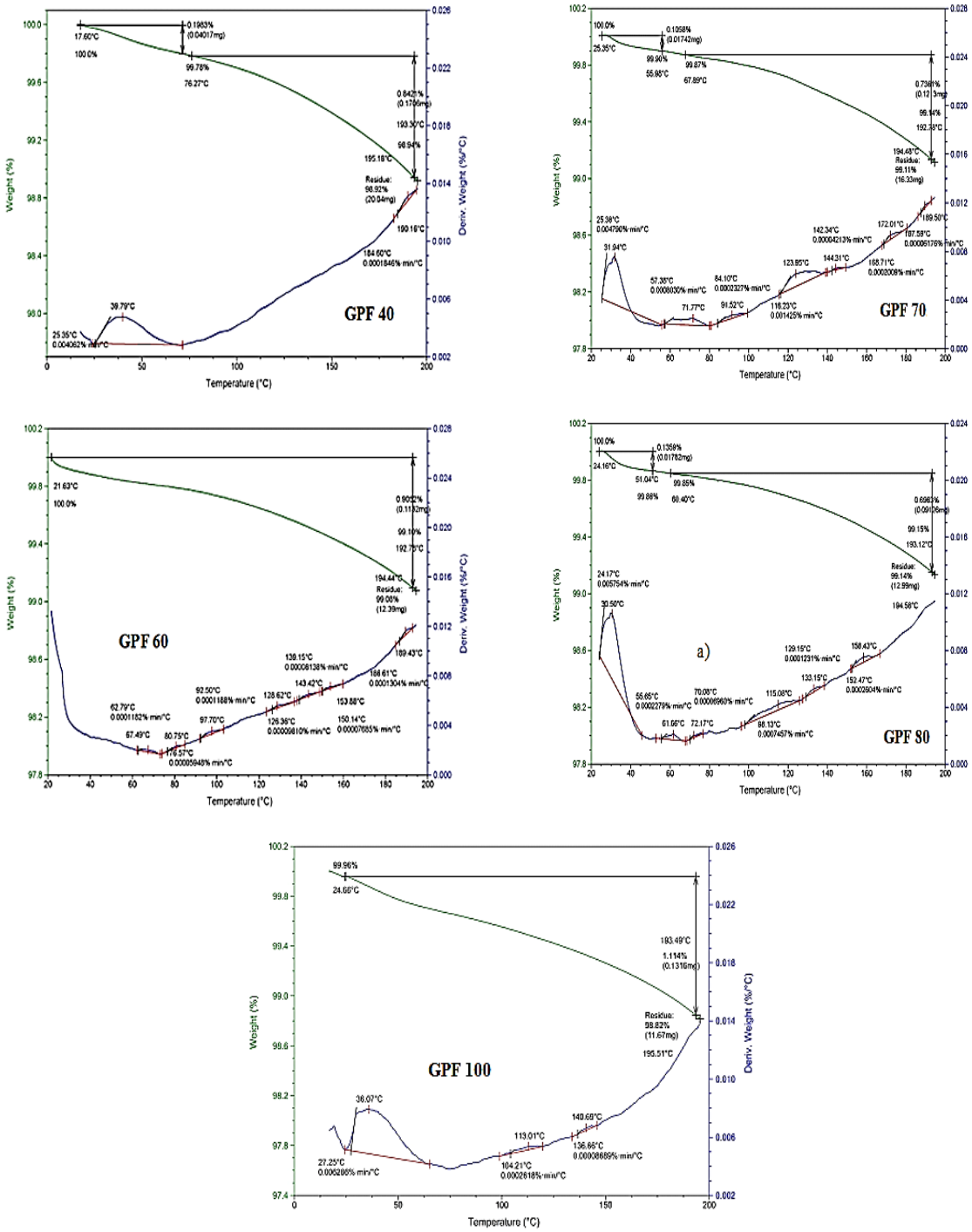

Figure 2. TGA thermographs for IIR/ GPF CB composite samples.

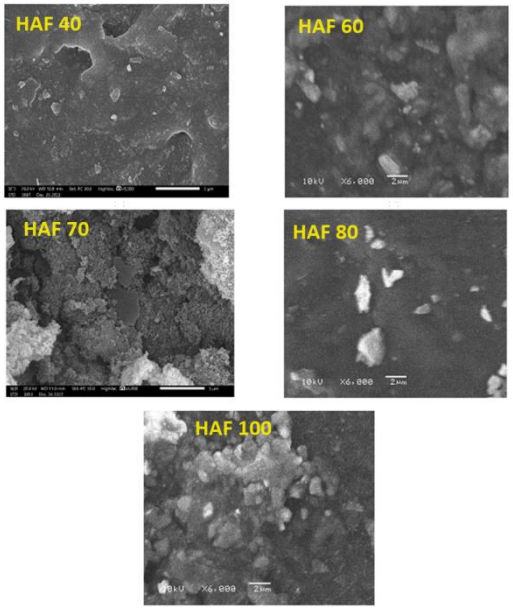

Figure 3. SEM images for IIR/HAF composite samples with resolution 6000X.

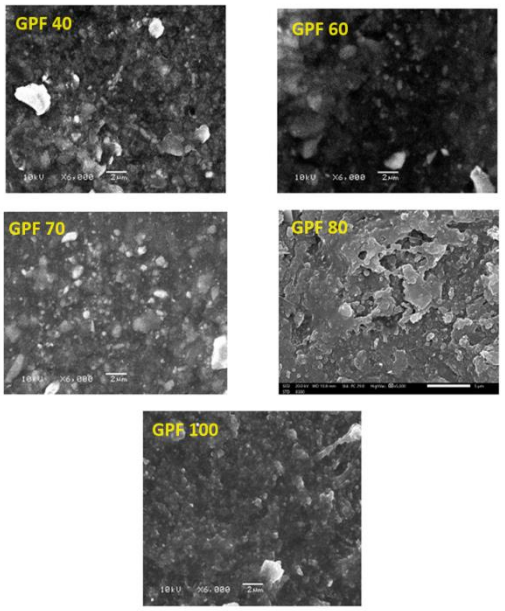

Figure 4. SEM images for IIR/GPF composite samples with resolution 6000X.

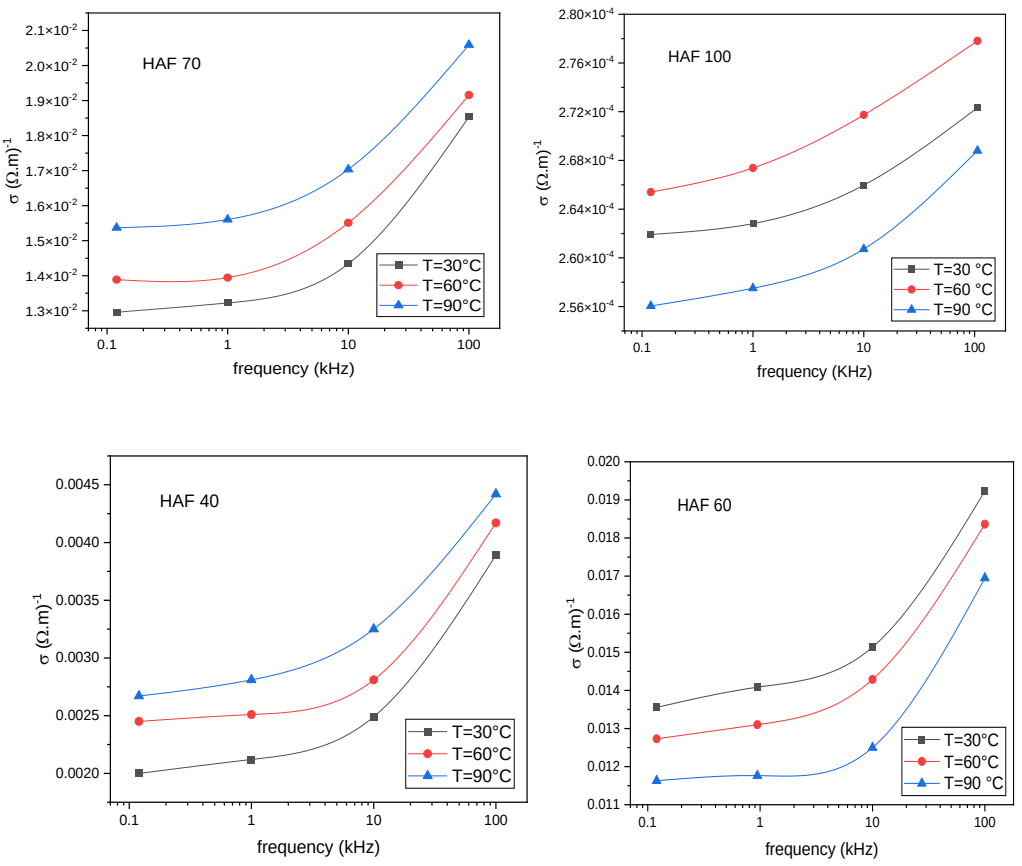

Figure 5. The variation of AC electrical conductivity with frequency at some selected temperatures for IIR/HAF CB samples.

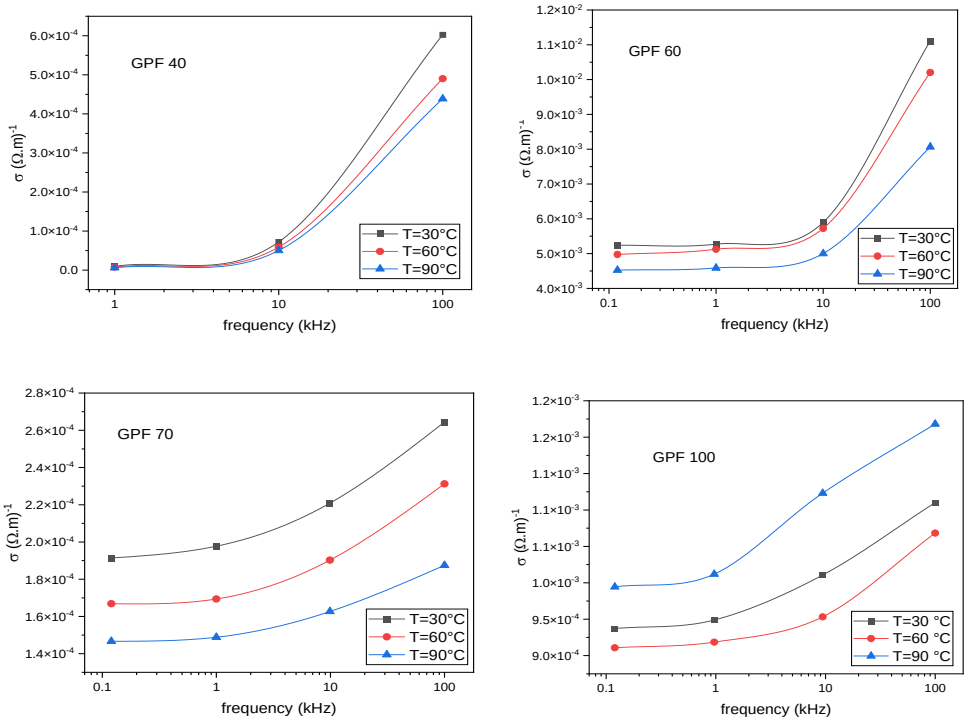

Figure 6. The variation of AC electrical conductivity with frequency at some selected temperatures for IIR/GPF CB samples.

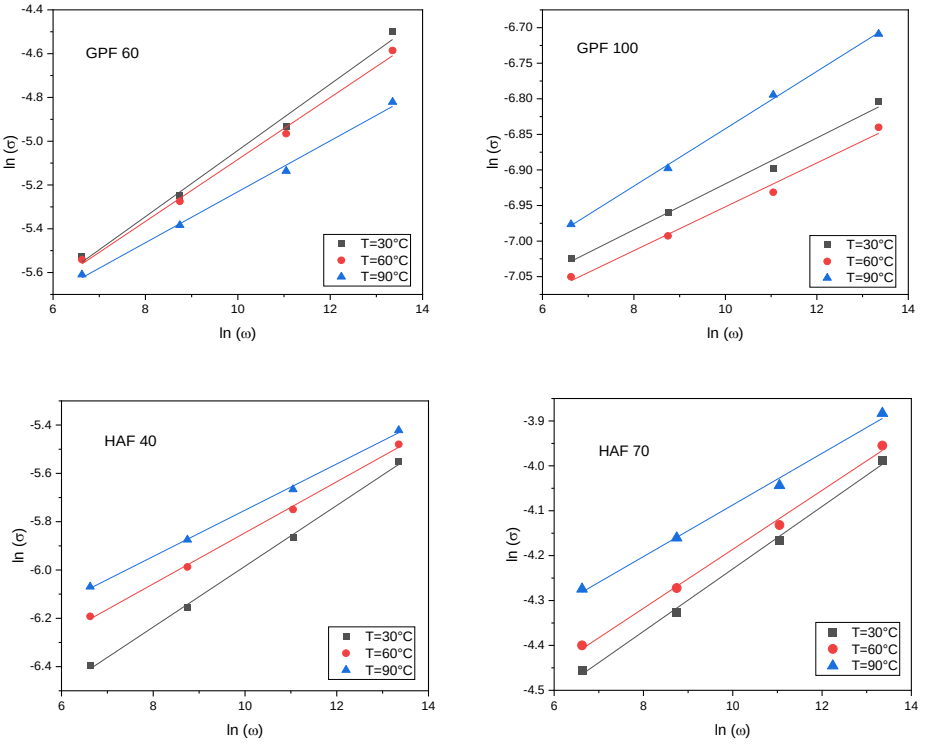

Figure 7. The variation of ln(σ) with ln(ω) for samples HAF 40, HAF 70, GPF 60 and GPF 100 at some selected temperatures.

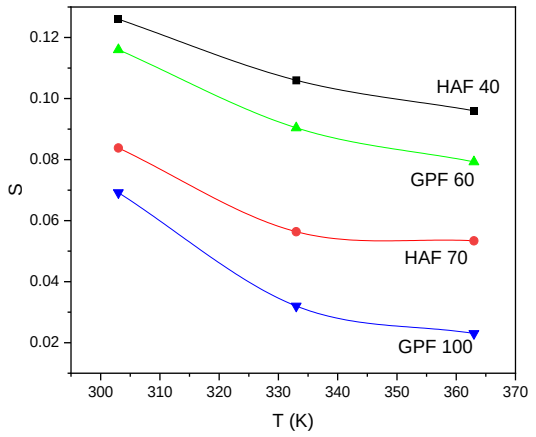

Figure 8. The variation of the exponent S with temperature for samples HAF 40, HAF 70, GPF 60 and GPF 100.

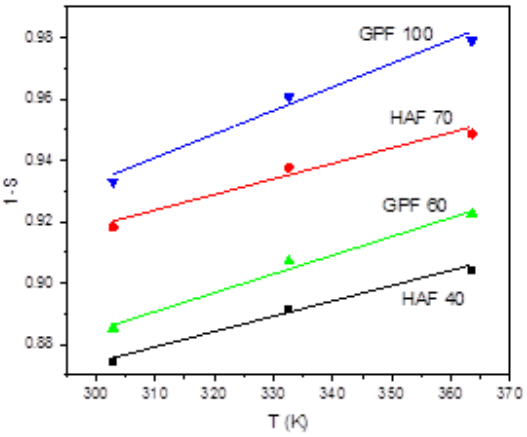

Figure 9. The variation of (1-S) with temperature for samples HAF 40, HAF 70, GPF 60 and GPF 100.

Table 2: Maximum barrier height in eV for samples HAF 40, HAF 70, GPF 60 and GPF 100

Sample	Maximum barrier height W_m (eV)
HAF 40	0.863
HAF 70	0.846
GPF 60	0.777
GPF 100	0.672

One of the important characteristics of the rubber/CB systems is the behavior of the dielectric constant with the temperature and frequency. The frequency dependence of relative dielectric constant (ε_r), dielectric loss (ε''), loss tangent ($\tan\delta$) were investigated for the IIR/carbon black composites.

The relative dielectric constant is obtained at various frequencies by using the measured capacitance (C) from the relation [30],

$$\varepsilon_r = \frac{C}{C_o} \qquad (4)$$

where C_o is capacitance of an empty capacitor. **Figure 10** shows the variation of the relative dielectric constant with the frequency for HAF and GPF samples at some selected temperatures.

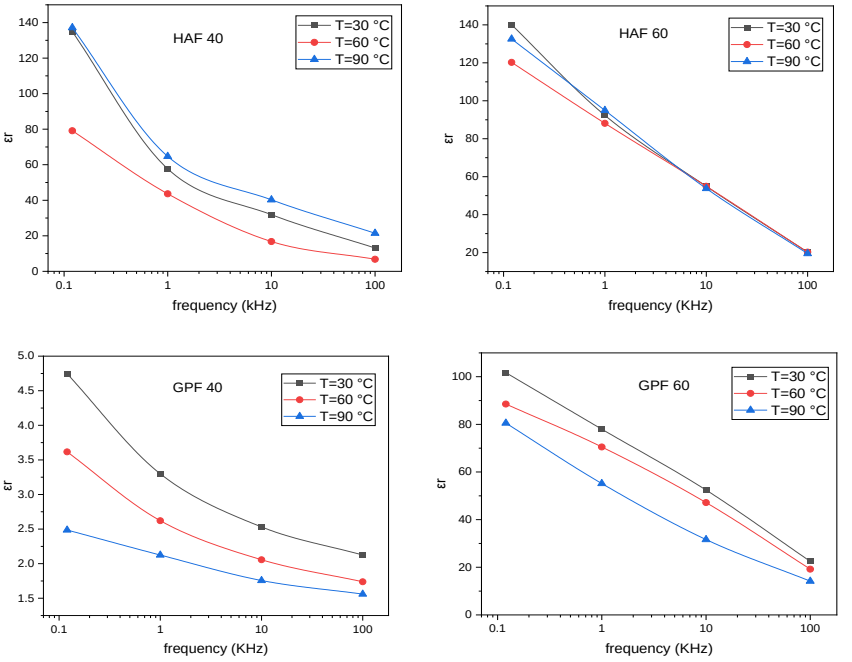

Figure 10. The variation of dielectric permittivity with frequency for samples HAF 40, HAF 60, GPF 40 and GPF 60.

Figure 10 reveals that ε_r decreases by increasing the frequency for all samples. This behavior is identical to that of dielectric materials against the driving external field. It was argued that the large values of ε_r, observed at low frequencies are due to the presence of filler content. The filler content, with the host matrix builds up interfacial capacitor, due to their inhomogeneous properties [31]. The formation of such interfacial capacitor will eventually increase the proposed interfacial polarization contribution to the dielectric response. Consequently, ε_r attains high values at low frequencies. On the other hand, at high frequencies, the polarity-varying time is small and therefore most of the charge carriers in the interfacial area cannot follow the driving field. Thus, the dielectric constant drops to lower values at higher frequencies [32]. Similar behavior was reported in typical semiconductors [33, 34].

The dielectric loss (ε''), which is the imaginary part of the complex permittivity, is calculated at various frequencies by using the measured conductance values (G) from the relation [30]

$$\varepsilon_r = \frac{C}{C_o} \tag{5}$$

where ω is the angular frequency of the ac signal. **Figure 11** demonstrates the variation of the dielectric loss with the frequency for HAF and GPF samples respectively at some selected temperatures.

It is observable that the dielectric loss continuously decreases by elevation of the ac frequency. This indicates that the oscillating carriers will slow their motion by the increase of the frequency where they are not capable to follow the oscillation of the field.

Moreover, the dielectric loss of the samples can be specified by the loss tangent given by

$$\tan\delta = \frac{\varepsilon''}{\varepsilon_r} \tag{6}$$

Figure 12 depicts the loss tangent as a function of frequency for some samples of IIR/HAF and IIR/GPF composites. The loss tangent behavior sharply decreases at low frequencies, then it tends to be nearly constant at high frequencies for the same reasons described above.

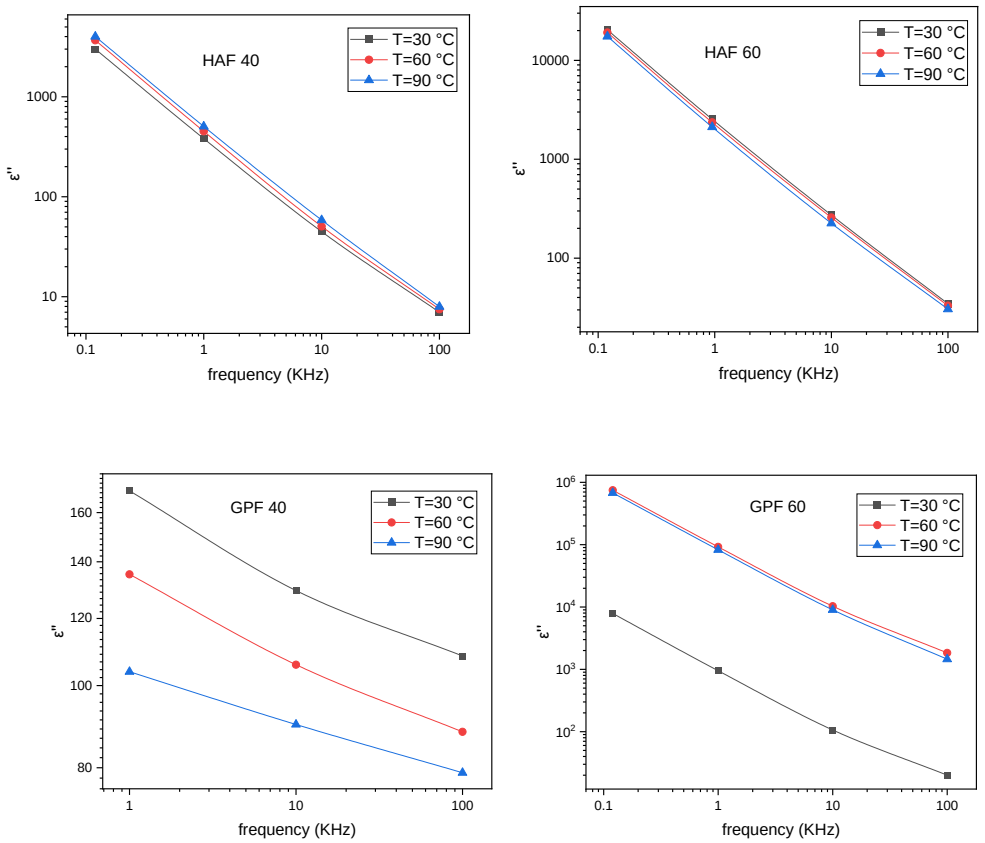

Figure 11. The variation of dielectric loss with frequency for samples HAF 40, HAF 60, GPF 40 and GPF 60.

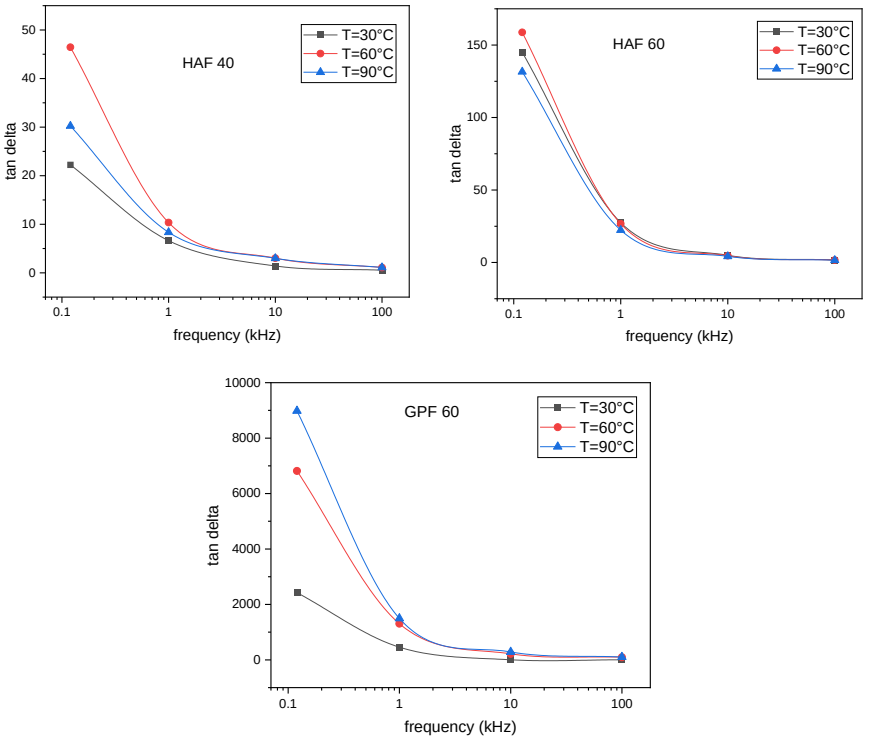

Figure 12. The variation of dielectric loss (tan δ) with frequency for samples HAF 40, HAF 60 and GPF 60.

4. Conclusions

Series of samples of isobutylene isoprene rubber filled with nano-sized HAF and GPF carbon black were synthesized. The structural, thermal, electrical and dielectric measurements were carried out for the prepared rubber/carbon black composites. The SEM photographs evidenced the distribution of the carbon black particles as aggregates inside the rubber. Thermal stability of the samples, examined using TGA, indicates that all rubber samples showed high stability within the range from room temperature up to 200 ºC. Frequency dependence of the AC conductivity was explained by corelated barrier hopping (CBH) process and the corresponding maximum barrier height was calculated. The results of dielectric permittivity, dielectric loss and loss tangent showed a decreasing behavior with the rise of the AC signal. Electrical measurements at lower temperature range are recommended.

Conflict of Interest

The authors declare that there is no conflict of interest regarding the publication of this paper.

References

[1] Kohjiya, S.; Ikeda, Y. A short history of natural rubber research. In: Kohjiya S, Ikeda Y, eds. Chemistry, Manufacture, and Applications of Natural Rubber. London: Elsevier; 2021. p.407-427.

[2] Cheremisinoff, N. P.; Cheremisinoff, P. N. Elastomer technology handbook, CRC Press, United States, 2020.

[3] Adelegan, O. J.; Coutant, Z. A.; Zhang, X.; Yamaner, F. Y.; Oralkan, Ö. Fabrication of 2D capacitive micromachined ultrasonic transducer (CMUT) arrays on insulating substrates with through-wafer interconnects using sacrificial release process. J. Microelectromechanical Syst. 2020, 29, 553-561.

[4] Manwar, R.; Islam, M. T.; Ranjbaran, S. M.; Avanaki, K. Transfontanelle photoacoustic imaging: ultrasound transducer selection analysis. Biomed. Opt. Express 2022, 13, 676-693.

[5] Zhao, Y.; Yang, W.; Tan, Y. J.; Li, S.; Zeng, X.; Liu, Z.; Tee, B. Highly conductive 3D metal-rubber composites for stretchable electronic applications. APL Mater. 2019, 7, 031508.

[6] Banerjee, P. S.; Rana, D. K.; Banerjee, S. S. Influence of microstructural alterations of liquid metal and its interfacial interactions with rubber on multifunctional properties of soft composite materials. Adv. Colloid Interface Sci. 2022, 308, 102752.

[7] Sreethu, T. K.; Naskar, K. Zinc oxide with various surface characteristics and its role on mechanical properties, cure-characteristics, and morphological analysis of natural rubber/carbon black composites. J. Polym. Res. 2021, 28, 183.

[8] Yadav, R.; Tirumali, M.; Wang, X.; Naebe, M.; Kandasubramanian, B. Polymer composite for antistatic application in aerospace. Def. Technol. 2020, 16, 107-118.

[9] Hazrati, K.; Sapuan, S.; Zuhri, M.; Jumaidin, R. Effect of plasticizers on physical, thermal, and tensile properties of thermoplastic films based on *Dioscorea hispida* starch. Int. J. Biol. Macromol. 2021, 185, 219-228.

[10] Düsenberg, B.; Tischer, F.; Seidel, A. M.; Kopp, S.-P.; Schmidt, J.; Roth, S.; Peukert, W.; Bück, A. Production and analysis of electrically conductive polymer – Carbon-black composites for powder based Additive Manufacturing. Procedia CIRP 2022, 111, 18-22.

[11] Vidakis, N.; Petousis, M.; Michailidis, N.; Mountakis, N.; Argyros, A.; Spiridaki, M.; Moutsopoulou, A.; Papadakis, V.; Charitidis, C. High-Density Polyethylene/Carbon Black Composites in Material Extrusion Additive Manufacturing: Conductivity, Thermal, Rheological, and Mechanical Responses. Polymers 2023, 15, 4717.

[12] Alves, A. M.; Cavalcanti, S. N.; da Silva, M. P.; Freitas, D. M. G.; Agrawal, P.; de Mélo, T. J. A. Electrical, rheological, and mechanical properties copolymer/carbon black composites. J. Vinyl Addit. Technol. 2021, 27, 445-458.

[13] Alfaramawi, K. Optical characteristics of butyl rubber loaded with general purpose furnace (GPF) carbon black. Mater. Res. Express. 2018, 5, 066202.

[14] Alfaramawi, K. Optical and dielectric dispersion parameters of general purpose furnace (GPF) carbon black reinforced butyl rubber. Polym. Bull. 2018, 75, 5713-5730.

[15] Jeddi, J.; Katbab, A. A.; Mehranvari, M. Investigation of microstructure, electrical behavior, and EMI shielding effectiveness of silicone rubber/carbon black/nanographite hybrid composites. Polym. Compos. 2019, 40, 4056-4066.

[16] Huang, M.; Tunnicliffe, L. B.; Liao, S.; Yang, B.; Yan, H.; Busfield, J. J. C. Broadband Dielectric Characterization of Carbon Black-Reinforced Natural Rubber. Rubber Chem. Technol. 2023, 96, 656–666.

[17] Kim, G. H.; Moon, Y. I.; Jung, J. K.; Choi, M. C.; Bae, J. W. Influence of Carbon Black and Silica Fillers with Different Concentrations on Dielectric Relaxation in Nitrile Butadiene Rubber Investigated by Impedance Spectroscopy. Polymers (Basel) 2021, 14, 155.

[18] Zhang, Q.; Wang, J.; Zhang, B.-Y.; Guo, B.-H.; Yu, J.; Guo, Z.-X. Improved electrical conductivity of polymer/carbon black composites by simultaneous dispersion and interaction-induced network assembly. Compos. Sci. Technol. 2019, 179, 106-114.

[19] Alfaramawi, K.; Abboudy, S.; Abulnasr, L.; Haridy, A. Electrical Conduction Mechanisms in Synthesized Ethylene Propylene Diene Monomer Rubber Loaded with High Abrasion Furnace Carbon Black. Indian J. Pure Appl. Phys. 2021, 59, 731-739.

[20] Alzamil, M.; Alfaramawi, K.; Abboudy, S.; Abulnasr, L. Electrical conduction hysteresis in carbon black–filled butyl rubber compounds. Int. J. Mod. Phys. B. 2018, 32, 1850100.

[21] Nguyen, D. H.; Sylvestre, A.; Gonon, P.; Rowe, S. Dielectric properties analysis of silicone rubber, Proceedings of the 2004 IEEE International Conference on Solid Dielectrics, 2004.

[22] Elliott, S. R. A.C. conduction in amorphous chalcogenide and pnictide semiconductors. Adv. Phys. 1987, 36, 135-217.

[23] Pike, G. E. AC Conductivity of Scandium Oxide and a New Hopping Model for Conductivity. Phys. Rev. B 1972, 6, 1572-1580.

[24] Elliott, S. R. A theory of A.C. conduction in chalcogenide glasses. Phil. Mag. 1977, 36, 1291-1304.

[25] Abboudy, S.; Ahmed, M.; El-Ata, A. A. AC multiple hopping conduction in Ni-Mn spinel magnetic ferrites. Phys. Low-Dim. Struct. 2001, 5, 105-116.

[26] Abboudy, S. AC Magneto-Conductance in n-InP in the Hopping Regime. Phys. Low-Dim. Struct. 2001, 93-106.

[27] Abboudy, S.; P., F.; R., M.; and Lea, M. J. Finite frequency scaling of hopping conductivity in n-InSb. Philos. Mag. Lett. 1988, 57, 277-282.

[28] Abboudy, S.; Mansfield, R.; Fozooni, P. AC conduction in n-type InSb in the magnetic freeze-out region. In: Landwehr G, ed. Proceedings of the international Conference; Applications of High Magnetic fields in Semiconductor Physics: Springer-Verlag Series in Solid State Science; 1992. p.482-487.

[29] Abboudy, S.; Alfaramawi, K.; Abulnasr, L. AC hopping conduction in lightly doped inP at low temperatures. Mod. Phys. Lett. B. 2013, 28, 1450002.

[30] Tataroğlu, A.; Yücedağ, İ.; Altindal, Ş. Dielectric properties and AC electrical conductivity studies of MIS type Schottky diodes at high temperatures. Microelectron. Eng. 2008, 85, 1518-1523.

[31] Hendi, A. Structure, electrical conductivity and dielectric properties of bulk, 2-amino-(4, 5-diphenylfuran-3-carbonitrile). Life Sci. J. 2011, 8, 554-559.

[32] El Nahrawy, A. M.; Ali, A. I.; Mansour, A. M.; Abou Hammad, A. B.; Hemdan, B. A.; Kamel, S. Talented Bi0.5Na0.25K0.25TiO3/oxidized cellulose films for optoelectronic and bioburden of pathogenic microbes. Carbohydr. Polym. 2022, 291, 119656.

[33] Abboudy, S.; Alfaramawi, K.; Abulnasr, L. Dielectric constant of moderately doped InP at low frequencies and temperatures. Eur. Phys. J. Plus. 2016, 131, 39.

[34] Abboudy, S. Low-temperature, low-frequency dielectric constant of lightly doped n-InP at high magnetic fields. Phys. B Condens. Matter. 1993, 184, 236-240.